

---

## On the Interaction of Wind and Waves

P. A. E. M. Janssen, P. Lionello and L. Zambresky

*Phil. Trans. R. Soc. Lond. A* 1989 **329**, 289-301

doi: 10.1098/rsta.1989.0077

---

### Email alerting service

Receive free email alerts when new articles cite this article - sign up in the box at the top right-hand corner of the article or click [here](#)

---

To subscribe to *Phil. Trans. R. Soc. Lond. A* go to: <http://rsta.royalsocietypublishing.org/subscriptions>

---

## On the interaction of wind and waves

BY P. A. E. M. JANSSEN<sup>1</sup>, P. LIONELLO<sup>2</sup> AND L. ZAMBRESKY<sup>3</sup>†

<sup>1</sup>*Department of Oceanography, Royal Netherlands Meteorological Institute (KNMI) De Bilt, The Netherlands*

<sup>2</sup>*ISDGM, Venice, Italy*

<sup>3</sup>*GKSS, Geesthacht, F.R.G.*

We discuss the effect of wind-generated, gravity waves on the air flow. We study this example of resonant wave mean flow interaction using the quasi-linear theory of wind-wave generation (A. L. Fabrikant *Izv. atmos. ocean. Phys.* 12, 524 (1976); P. Janssen *J. Fluid Mech.* 117, 493–506 (1982)). In this theory both the effects of the waves and the effect of air turbulence on the mean wind profile is taken into account.

For a given wave spectrum, results of the numerical calculation of the steady-state wind profile are presented. The main result is that for young wind sea most of the stress in the boundary layer is determined by the transfer of momentum from wind to waves, therefore resulting in a strong coupling between air flow and waves. For old wind sea there is, however, hardly any coupling. As a consequence, a sensitive dependence of the aerodynamic drag on the wave age is found, explaining the scatter in plots of the experimentally observed drag as a function of the wind speed at 10 m. Also, the growth rate of waves by wind is found to depend on wave age, reflecting the effect of the waves on the wind profile.

All this suggests that a proper description of the physics of the momentum transfer from atmosphere to the ocean waves can only be given by coupling an atmospheric boundary-layer model with an ocean-wave prediction model. Here, we present the first results of the coupling of a simple surface-layer model with the third-generation wave model. The wave-induced stress is found to have a significant impact on the results for the wave height and the stress in the surface layer.

### 1. INTRODUCTION

Presently, there is interest in the problem of the coupling of wind and ocean waves. One reason is that knowledge of the sea state might improve our estimates of, for example, the momentum flux at the air–sea interface, as the wave-induced stress is a considerable fraction of the total stress in the surface layer (Komen 1985; Janssen 1988). A better knowledge of the momentum flux might be beneficial for wave prediction, storm-surge prediction and modelling of the climate.

In this paper, we discuss the physics of the interaction of wind and waves. Therefore, in §2 we present a model of the generation of waves by wind in which the shape of the wind profile is determined by both the turbulent stress and the wave-induced stress. For a given spectrum, the JONSWAP (1973) spectrum, we present results of the calculation of the steady-state wind profile and the dependence of both drag coefficient and the growth rate of waves by wind on the stage of development of the wind sea (measured by the wave-age parameter). Results are found to depend sensitively on the spectral shape of the high-frequency waves. The

† Present address: European Centre for Medium Range Weather Forecasts, Reading, Berkshire, U.K.

consequences of the wave-age dependence of the stress on wave prediction will be discussed in §3. To that end, we coupled a third-generation wave model (WAM) with a simple surface layer model. Results of numerical simulations show that under generating conditions (young-wind sea) a significant impact of the wave-stress on wave height and stress in the surface layer is to be expected.

## 2. QUASILINEAR THEORY OF WIND-WAVE GENERATION

In generating conditions the air flow over wind waves loses momentum to those waves. Thus, compared to air flow over a flat plate, the air flow over surface gravity waves experiences an additional stress, the so-called wave-induced stress  $\tau_w$ . Denoting by  $\tau_{\text{turb}}$  the turbulent stress and by  $\tau_{\text{visc}}$  the viscous stress, the steady-state momentum balance in air becomes (Janssen 1982),

$$\frac{\partial}{\partial z} \tau_{\text{turb}} + \frac{\partial}{\partial z} \tau_w + \frac{\partial}{\partial z} \tau_{\text{visc}} = 0, \quad (1)$$

where  $z$  denotes the height above the mean water surface. The turbulent stress  $\tau_{\text{turb}}$  will be modelled by means of a mixing length hypothesis,

$$\tau_{\text{turb}} = \rho_a l^2 \left| \frac{\partial}{\partial z} U_0 \right| \frac{\partial}{\partial z} U_0, \quad (2)$$

where  $U_0(z)$  is the wind profile,  $\rho_a$  is the air density and the mixing length  $l$  is given by  $l = \kappa z$  ( $\kappa$  is the von Karman constant).

The viscous stress is given by the usual expression

$$\tau_{\text{visc}} = \nu_a \frac{\partial}{\partial z} U_0,$$

where  $\nu_a$  is the kinematic viscosity of air.

For one-dimensional wave propagation, the wave-induced stress was determined by Fabrikant (1976) and Janssen (1982) (see also Miles 1965). The wave motion at the surface induces a secondary flow in the air and the vertical and horizontal components of this wave-induced flow give rise to the wave-induced stress  $\tau_w$ . In the quasi-linear approximation, only the transfer of momentum through an interaction between the wind and a single wave is considered. Multiple wave-wind interactions are disregarded. Therefore, assuming the validity of Miles's resonant wave-mean flow mechanism (1957) for the transfer of momentum from airflow to the waves, the wave-induced stress is then given by

$$\tau_w(z) = -\rho_a \int_z^\infty dz D_w \frac{\partial^2}{\partial z^2} U_0, \quad (3)$$

where the wave diffusion coefficient  $D_w$  is proportional to the wavenumber spectrum  $\phi(k)$ ,

$$D_w = \frac{\pi c^2 k^2 |\chi|^2}{|c - v_g|} \phi(k), \quad (4)$$

and  $c$  is the phase speed  $\omega/k$ ,  $\omega$  is the angular frequency,  $k$  the wave number and  $v_g$  is the group velocity  $\partial\omega/\partial k$  of the surface waves. The wave number  $k$  has to be expressed as a function of height through the resonance condition  $W = U_0(z) - c = 0$ . Finally,  $\chi$  is the normalized vertical component of the wave-induced air velocity that satisfies Rayleigh's equation

$$\{W[(\partial^2/\partial z^2) - k^2] - W''\} \chi = 0, \quad \chi(0) = 1, \quad \chi(\infty) \rightarrow 0, \quad (5)$$

where a prime denotes differentiation with respect to height  $z$ .

The loss of momentum from the air flow must, by conservation of momentum, be

accompanied by a growth of the water waves. As a result, the rate of change in time of the wavenumber spectrum because of wind is given by

$$\frac{\partial}{\partial t} \phi \Big|_{\text{wind}} = \gamma \phi, \quad \gamma = -\pi \epsilon c |\chi_c|^2 W_c'' / |W_c'|, \quad (6)$$

where the subscript c refers to evaluation at the critical height  $z_c$  defined by  $W = 0$  and  $\epsilon$  is the ratio of air to water density  $\rho_w$ . Here, conservation of momentum is expressed by the relation (Janssen 1988)

$$\tau_w(z=0) = \rho_w \int_0^\infty dk \omega \frac{\partial \phi}{\partial t} \Big|_{\text{wind}}, \quad (7)$$

in other words, the wave-induced stress on the airflow is given by the rate of change due to wind of the total wave momentum

$$P = \rho_w \int_0^\infty dk \omega \phi. \quad (8)$$

Equation (7) is useful in giving an estimate of the total wave-induced stress, provided the growth rate  $\gamma$  of the waves by wind and the wave spectrum are known. As we are mainly interested in the contribution to the stress of the longer, low-frequency waves, a reliable, empirical expression for the growth rate  $\gamma$  of the waves by wind is given by (Komen *et al.* 1984)

$$\gamma = \mu \epsilon \omega (28u_* / c - 1). \quad (9)$$

Here, we assumed propagation of the waves in the direction of the wind and  $u_*$  is the friction velocity, where  $u_* = (\tau / \rho_a)^{1/2}$  with  $\tau$  the total stress. From the Bight of Abaco data, Snyder *et al.* (1981) infer for  $\mu$  a mean value of 0.25. For the spectrum, we use the simple shape

$$\phi(k) = \begin{cases} 0, & k < k_p, \\ \frac{1}{2} \alpha_p k^{-3}, & k > k_p, \end{cases} \quad (10)$$

where  $k_p$  is the peak wave number corresponding to the peak frequency  $\omega_p = \sqrt{gk_p}$  and  $\alpha_p$  is the Phillips constant. The  $k^{-3}$  power law was first proposed by Phillips (1958) and is based on wave breaking being the dominant limiting mechanism for the wave spectrum. Substitution of (9) and (10) into equation (7) gives as a first estimate for the ratio of wave-induced stress to total stress  $\rho_a u_*^2$ ,

$$\tau_w / \rho_a u_*^2 = \mu \alpha_p [28c_p / u_* - \frac{1}{2}(c_p u_*)^2], \quad (11)$$

where  $c_p$  is the phase speed at the peak of the spectrum and the quantity  $c_p / u_*$  is called the wave age. The wave age is a measure for the stage of development of wind sea. Typical values are  $c_p / u_* \approx 5$  for young wind sea and  $c_p / u_* > 25$  for old wind sea. The Phillips constant  $\alpha_p$  is according to the JONSWAP field data (1973) a function of wave age. Following Snyder (1974) we take

$$\alpha_p = 0.57 (c_p / u_*)^{-3/2}. \quad (12)$$

The result is a wave-induced stress, as shown in figure 1, that is large for young-wind sea while small for old wind sea. This is in agreement with one's intuition that air flow over young wind sea is rougher than over old wind sea, and it is supported by measurements at sea (Donelan 1982). It should be noted, however, that the behaviour of the wave stress as a function of wave age depends sensitively on how the high-frequency part of the spectrum depends on wave age (Janssen 1988).

From figure 1 it is evident that the wave stress is a considerable fraction of the total stress in the surface layer, in particular for young wind sea. It is therefore relevant to determine the effect of the waves on the wind profile, on the drag coefficient and as a consequence on the

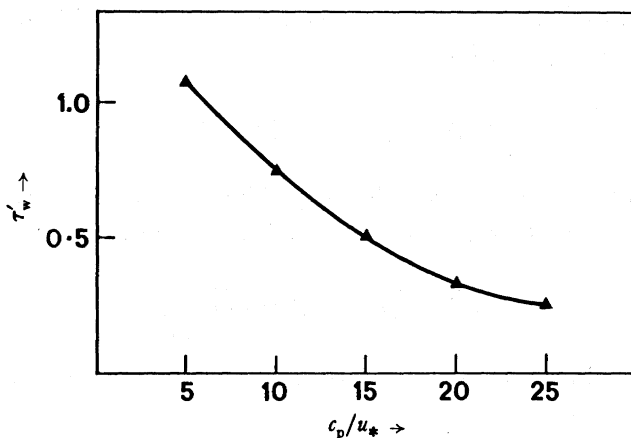


FIGURE 1. Dimensionless wave stress  $\tau'_w = \tau_w / \rho_a u_*^2$  as a function of wave age.

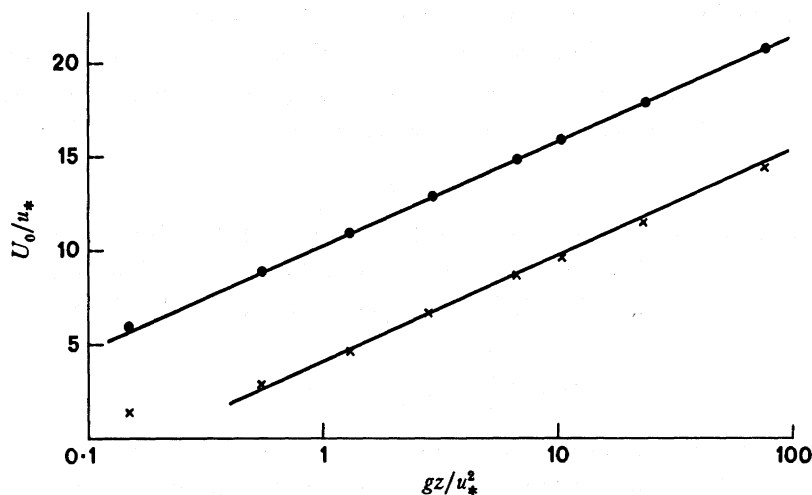


FIGURE 2. Steady-state wind profile as a function of dimensionless height for young wind sea ( $\times$ ),  $c_p/u_* = 5$ , and for old wind sea ( $\bullet$ ),  $c_p/u_* = 25$ ;  $u = 0.7 \text{ m s}^{-1}$ .

growth rate of the waves. To this end the set of equations (1)–(5) was solved on the computer by Janssen (1988), where the growth rate  $\gamma$  of the waves was determined by (6). Before we present the results, however, the limitations of this model should be realized. It only applies for those waves that have their critical layer outside the viscous sublayer in the air. In other words, the expression for the diffusion coefficient is only valid for the longer waves with  $c/u_* > 5$ . Still, it is important to take the effect of the short waves (gravity-capillary range) on the wind profile into account as well. We model the momentum loss from wind to these short waves by means of the introduction of a roughness length  $z_0$ , i.e. we impose on  $z = z_0$  the boundary condition

$$U(z = z_0) = 0 \tag{13}$$

where  $z_0$  is given by Charnock's relation (1955)

$$z_0 = \alpha u_*^2 / g, \quad \alpha = 0.0144. \tag{14}$$

For large height  $z$  we assume that the effect of the waves on the wind may be neglected so that  $\tau = \tau_{\text{turb}}$ . As a result we find the boundary condition

$$\tau_{\text{turb}} = \rho_a u_*^2 \quad (z \rightarrow \infty). \tag{15}$$

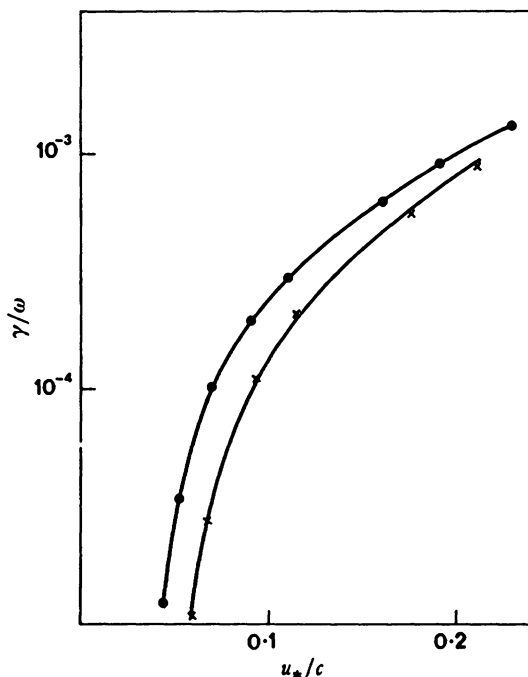


FIGURE 3. Growth rate  $\gamma/\omega$  of the waves as a function of  $u_*/c$ . Symbols: ●,  $c_p/u_* = 25$ ; ×,  $c_p/u_* = 5$ ;  $u_* = 0.7 \text{ m s}^{-1}$ .

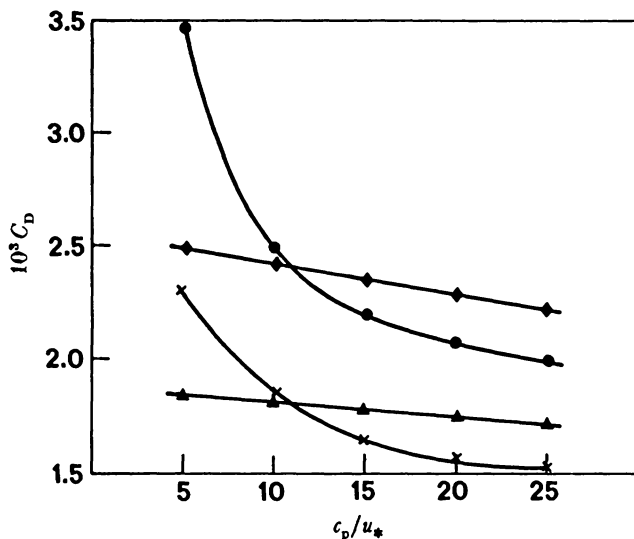


FIGURE 4. Wave age dependence of drag coefficient for two friction velocities. Symbols: for  $\alpha_p \approx c_p^{1/4}$ , ×,  $u_* = 0.3 \text{ m s}^{-1}$ ; ●,  $u_* = 0.7 \text{ m s}^{-1}$ ; for  $\alpha_p \approx c_p^{1/3}$ , ▲,  $u_* = 0.3 \text{ m s}^{-1}$ ; ◆,  $u_* = 0.7 \text{ m s}^{-1}$ .

The equations (1)–(5) supplemented by the boundary conditions (13)–(15) were numerically solved by Janssen (1988). We merely quote the relevant results for the JONSWAP spectrum

$$\left. \begin{aligned} \phi(k) &= \frac{1}{2} \alpha_p k^{-3} \exp \left\{ -\frac{5}{4} (k_p/k)^2 \right\} \gamma^r, \\ r &= \exp \left\{ -\frac{1}{2} [(\sqrt{k} - \sqrt{k_p}) / \sigma \sqrt{k_p}]^2 \right\}, \end{aligned} \right\} \quad (16)$$

where  $\alpha_p$  is the Phillips constant as given by equation (12),  $\gamma$  is the peak enhancement and  $\sigma$

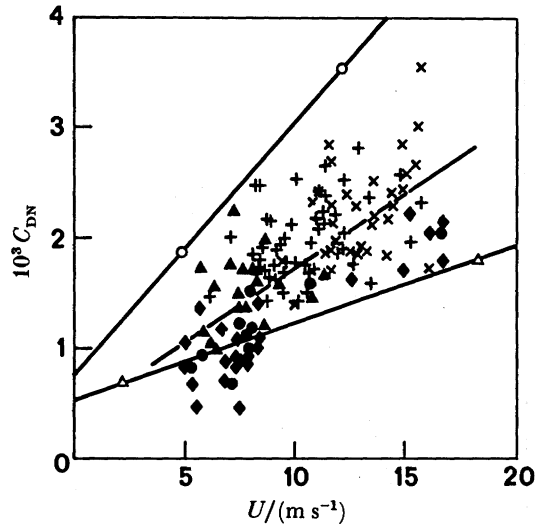


FIGURE 5. Observed neutral drag coefficient as a function of wind speed at 10 m, stratified according to wave age  $U/c_p$  (from Donelan 1982). Symbols:  $\blacklozenge$ ,  $0.8 < u/c_p < 1.5$ ;  $\bullet$ ,  $1.5 < u/c_p < 2.0$ ;  $\blacktriangle$ ,  $2.0 < u/c_p < 3.0$ ;  $+$ ,  $3.0 < u/c_p < 4.0$ ;  $\times$ ,  $4.0 < u/c_p < 6.0$ ;  $\circ$ ,  $u_*/c_p = 0.2$ ;  $\triangle$ ,  $u_*/c_p = 0.04$ .

is the width of the spectral peak. For simplicity, we shall give  $\gamma$  and  $\sigma$  the constant values 3.3 and 0.10, respectively, and  $k_p = g/c_p^2$ .

For old wind sea ( $c_p/u_* = 25$ ) hardly any effect of the waves on the wind profile and the growth rate of surface waves is found as the wave-induced stress is only a small fraction of the total stress. However, young wind sea shows a significant impact of the sea state on both the wind profile and the growth rate of the waves as illustrated by figure 2 (plot of windspeed) and figure 3 (plot of dimensionless growth rate against  $c/u_*$ ). As a consequence, the drag coefficient at 10 m is a sensitive function of wave age, which is shown in figure 4. The major result we find is that we can explain the large scatter in plots of the observed drag coefficient as a function of the windspeed at 10 m. As an example, consider the field data obtained by Donelan (1982) that are displayed in figure 5. These data are stratified according to wave age and they show a considerable scatter. In addition, we have shown in figure 5 lines of constant wave age according to the present theory. This clearly offers an explanation of the observed scatter.

### 3. ON THE COUPLED OCEAN-WAVE, ATMOSPHERE MODEL

A considerable fraction of the stress in the atmospheric boundary layer is carried by ocean waves, especially for young wind sea. In the previous section we found that the aerodynamic drag of sea waves is a sensitive function of wave age, where the wave spectrum was given by the JONSWAP shape with a Phillips constant  $\alpha_p$  depending sensitively on wave age.

We now ask what happens when the wave spectrum is allowed to evolve according to the dynamics of the energy balance equation. Do we still obtain a sensitive dependence of the aerodynamic drag on the wave age? This question is important because, if the drag would be more or less independent of the sea state, coupling of an atmospheric boundary-layer model with an ocean-wave model would be meaningless, despite the fact that the wave-induced stress is a considerable fraction of the total stress. Seen from the view point of atmospheric modellers, a simple parametrization of the wave-induced stress would suffice. However, the careful

observations of Donelan (1982) show a considerable dependence of the aerodynamic drag on the sea state, suggesting that coupling of an atmospheric boundary-layer model and a wave model is indeed meaningful. Therefore, the results of our coupling experiment should give a sensitive wave-age dependence of the drag over ocean waves.

The boundary-layer equations we used take only the effects of turbulent and wave-induced stress on the momentum balance into account. Integrating over a layer with thickness  $\Delta z_i$ , where  $i$  denotes the  $i$ th layer we have

$$\frac{\partial}{\partial t} U_i = \frac{\tau_{i+1} - \tau_i}{\Delta z_i}, \quad (17)$$

where  $U_i$  is the average windspeed. Away from the surface layer ( $i \geq 1$ ) the stress  $\tau_i$  is given by (here, and in the rest of the paper we divide the stress by  $\rho_a$ )

$$\tau_i = K_i (\Delta U_i / \Delta z_i), \quad (18)$$

where  $\Delta U_i = U_i - U_{i-1}$ ,  $K_i = l_i^2 |\Delta U_i / \Delta z_i|$  and  $l_i$  is the so-called mixing length,

$$l(z) = \kappa z / (1 + \kappa z / \lambda), \quad (19)$$

with  $\kappa$  the von Karman constant, and where we introduced the length scale  $\lambda$  to prevent the size of the eddies from growing indefinitely for large height  $z$ . We took  $\kappa = 0.41$ ,  $\lambda = 100$  m,  $\Delta z_i = 20$  m and the number of layers  $N$  was 10 so that the top of our boundary layer is at 200 m.

At the surface ( $i = 0$ ) the stress is given by

$$\tau_0 = C_D(U_0) |U_0| U_0 + \tau_w, \quad (20)$$

where  $\tau_w$  is the wave-induced stress that will be determined from the wave-model spectrum and the first term models the combined loss of momentum owing to viscous dissipation and the growth of gravity-capillary waves. The drag coefficient  $C_D$  is given by

$$C_D = (0.8 + 0.065 U_0) 10^{-3}. \quad (21)$$

A similar dependence of  $C_D$  on wind speed is found by using a logarithmic wind profile with the Charnock relation for the roughness length (Wu 1982).

In the coupling experiment we assumed that because of changes in the surface stress the wind field relaxes almost instantly to the new equilibrium. This is a reasonable assumption as a typical timescale  $T$  in the surface layer is given by  $T \approx l_0 / u_* < 1$  min for  $l_0 = 20$  m and  $u_* \approx 0.5$ – $1$  m s<sup>-1</sup> whereas a typical timescale for the wave field is of the order of 15 min. We consider unidirectional wind fields only, i.e. the wind direction does not change in time and space. From the condition of constant stress one then finds the following relation between the wind speed at the top of the boundary layer,  $U_N$ , and the surface wind speed

$$U_0 = U_N - \tau_0^{\frac{1}{2}} \sum_{i=1}^N \Delta z_i / l_i, \quad (22)$$

where  $\tau_0$  depends on the surface wind speed  $U_0$  and the wave-induced stress  $\tau_w$  (cf. equation (20)). Thus, for given wind speed  $U_N$  and given wave-induced stress  $\tau_w$ , one can solve (22) for  $U_0$  and one obtains the total stress at the surface using (20).



Let us now turn to the determination of the wave stress  $\tau_w$ . For waves propagating in two dimensions the wave stress is defined by

$$\tau_w = (\rho_w/\rho_a) \int df d\theta \omega l \left. \frac{\partial}{\partial t} F \right|_{\text{wind}}, \quad l = k/k, \quad (23)$$

where the evolution of the two-dimensional frequency spectrum  $F(f, \theta)$  is determined by the energy balance equation (WAMDI-group 1988)

$$\frac{\partial}{\partial t} F + \mathbf{v}_g \cdot \frac{\partial}{\partial \mathbf{x}} F = S = S_{\text{in}} + S_{\text{nl}} + S_{\text{ds}}, \quad (24)$$

where  $\mathbf{v}_g$  is the group velocity  $\partial\omega/\partial\mathbf{k}$  and the source terms describe the physics of the generation of surface waves by wind ( $S_{\text{in}}$ ), nonlinear four-wave processes ( $S_{\text{nl}}$ ) and dissipation due to white capping.

The nonlinear interactions are determined by means of the discrete interaction approximation (S. Hasselmann *et al.* 1985). The wind input term is, according to our results of the previous section, both a function of the dimensionless phase speed  $c/u_*$  and the sea state, which is determined by either the wave age  $c_p/u_*$  or the local steepness of the spectrum. We preferred the last measure for the sea state, so that we assume that the wind input term also depends on the steepness parameter

$$s = \omega k^2 F / 2\pi,$$

which for the  $f^{-5}$  spectrum (cf. equation (10)) is just equal to the Phillips constant  $\alpha_p$ .

We therefore modified  $S_{\text{in}}$  to

$$S_{\text{in}} = \mu \epsilon \omega [28 Q u_* / c \cos(\theta - \phi) - 1] F, \quad (25)$$

where  $\phi$  is the wind direction and the factor  $Q = Q(s)$  reflects the change of the wave growth rate owing to the effect of the waves on wind. Based on the results of figure 3 we find

$$Q = 1/(1 + \Delta), \quad \Delta = 28\alpha s \quad (26)$$

with  $\alpha \approx 0.3$ . The case  $Q = 1$  corresponds to the wind input term of the standard WAM model. The dissipation source function is linear in the wave spectrum with a coefficient that depends on the wave energy  $E$ , mean wave number  $\langle k \rangle$  and mean angular frequency  $\langle \omega \rangle$ ,

$$S_{\text{ds}} = -\beta \langle \omega \rangle (\langle k \rangle^2 E)^2 [k/\langle k \rangle]^m F, \quad (27)$$

where

$$E = \int df d\theta F$$

and  $\langle k \rangle$  and  $\langle \omega \rangle$  are averages with the spectrum  $F$  as weight (cf. WAMDI-group 1988). The standard WAM model has  $\beta = 2.6$  and  $m = 1$ . Here, we would like to study the dependence of results for wave height  $H_s = 4\sqrt{E}$ , Phillips constant  $\alpha_p$ , wave stress  $\tau_w$  on parameters  $\beta$  and  $m$ .

The energy balance equation (24) is solved for  $F$  in a finite frequency domain  $D$  only. This domain is defined by

$$D: 0.0418 < f < \min(f_c, 0.4114), \quad (28)$$

where in the standard WAM  $f_c$  is given by the maximum of  $2.5 \langle \omega \rangle / 2\pi$  and  $4 f_{\text{PM}}$ , whereas in the coupled run we took  $f_c = 0.4114$ . For frequencies larger than  $f_c$  we assume an  $f^{-5}$  tail where the directional distribution is determined by the one at  $f = f_c$ . Wave energy, mean wavenumber, mean frequency and the wave-induced stress are then determined by an

integration over the full frequency range. Incidentally, the standard wave model assumes an  $f^{-4}$  high-frequency tail. However, for the wave stress this would give rise to a logarithmic singularity at high frequencies.

Because observations also seem to favour an  $f^{-5}$  power law (Birch & Ewing 1986; Forristal 1981; Banner 1988), we decided to use this power law for the high-frequency part of the spectrum. To avoid any misunderstandings it should be emphasized that the results of the standard wave model are insensitive to the choice of the high-frequency tail. When this model is, however, coupled to a boundary-layer model, the choice of the high-frequency tails matters, as the wave stress (which effects the total stress through equation (20)) is sensitive to details of the high-frequency part of the spectrum.

We performed numerical experiments with a one grid point version of this coupled wave-surface layer model, which we implemented on a personal computer (AT with co-processor). Therefore, we only report results of wave height, Phillips constant  $\alpha_p$  and wave stress on duration. These are displayed in the figures 6, 7 and 8. The initial condition was a JONSWAP spectrum with wave-age  $c_p/u_* = 5$  and a  $\cos^2$  directional distribution. The energy balance equation was integrated for 12 directions and 25 frequencies (on a logarithmic scale, 0.0418–0.4114). The integration time step for the waves was 3 min whereas wind and waves were coupled every 15 min so that there was sufficient time for the wind to relax to a new equilibrium. The wind speed  $U_N$  at the top of the boundary layer was chosen to be  $U_N = 26.83 \text{ m s}^{-1}$ , corresponding, in the absence of waves, to a friction velocity of  $u_* = 0.85 \text{ m s}^{-1}$ .

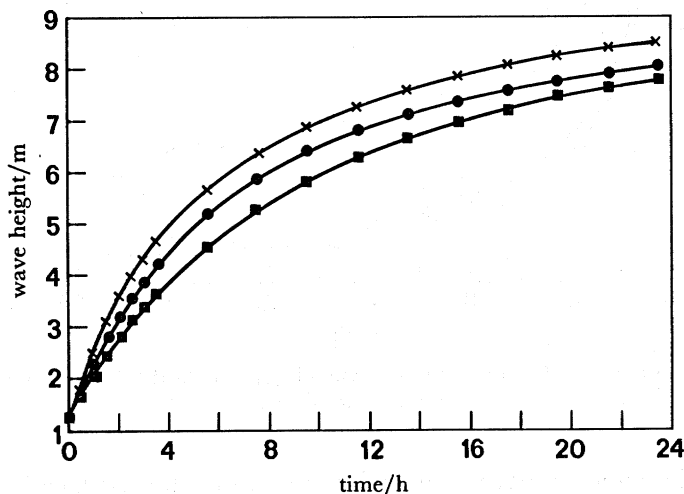


FIGURE 6. Wave height against time for standard wave model and coupled-wave, surface-layer model. Symbols =  $\blacksquare$ , standard WAM;  $\times$ , coupled ( $\alpha = 0.1$ ); coupled ( $\alpha = 0.4$ ).

The first numerical experiment we did was a run with the standard version of the wave model without any coupling between wind and waves. Thus, we took  $\alpha = 0$  (no effect of waves on wind), in the expression for the dissipation we used  $\beta = 2.6$  and  $m = 1$ , and we disregarded the wave-induced stress in the determination of the stress. The corresponding results in the figures 6, 7 and 8 are denoted by the square ( $\blacksquare$ ) symbol. It is evident from figure 7 that for this case the wave-induced stress is fairly constant so that there is hardly any dependence on the growth stage of the waves. Also, the Phillips constant  $\alpha_p$  assumes, even for large duration, fairly large values.

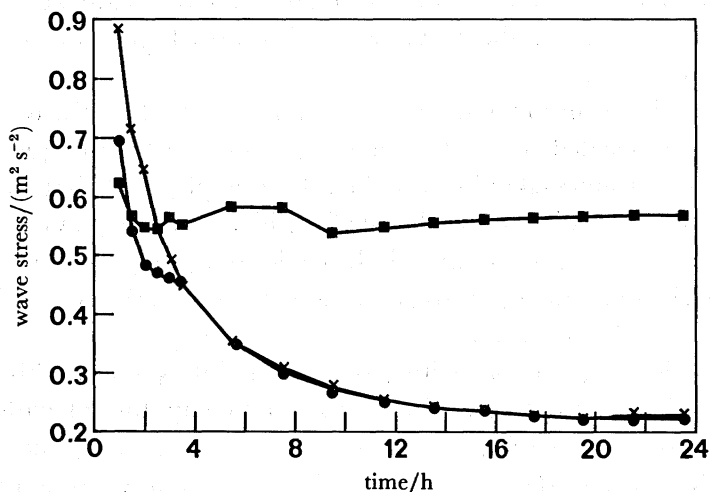


FIGURE 7. Wave-induced stress as a function of time. Symbols: ■, standard WAM; ×, coupled ( $\alpha = 0.1$ ); ●, coupled ( $\alpha = 0.4$ ).

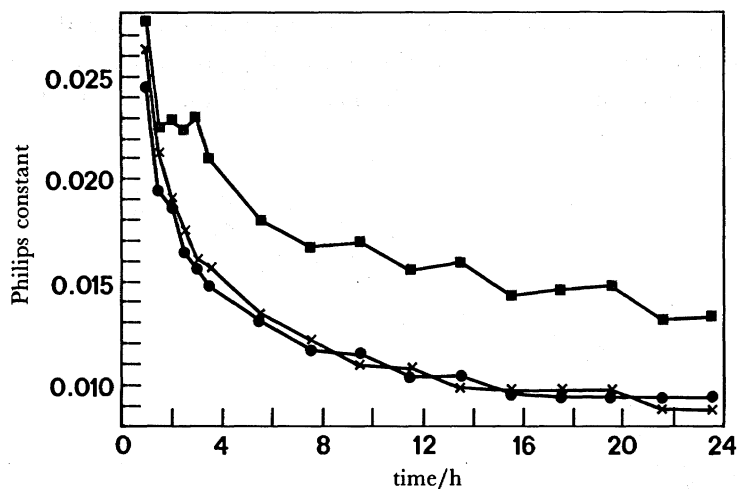


FIGURE 8. Phillips constant as a function of time. Symbols: ■, standard WAM; ×, coupled ( $\alpha = 0.1$ ); ●, coupled ( $\alpha = 0.4$ ).

Next, we coupled the standard WAM model with our steady-state surface-layer model and we found similar unsatisfactory behaviour of the wave-induced stress as a function of duration. Including the effect of the waves on the wind profile (e.g. finite  $\alpha$ ) did not remedy this problem as this effect is only important for the early stages of wave growth. Because the wave-induced stress is so sensitive to details of the high-frequency part of the wave spectrum, we decided to increase the effect of dissipation in that part of the spectrum. We therefore performed experiments with  $m = 2$  and  $m = 3$  while keeping  $\beta = 2.6$ . Results with  $m = 3$  gave too low values of the Phillips constant  $\alpha_p$  for long duration, whereas  $m = 2$  gave satisfactory results. We therefore only discuss results with  $m = 2$ .

The dissipation due to whitecapping in the standard wave model (hence  $m = 1$ ) is based on Hasselmann (1974). In this theory, it is argued that whitecapping is a process that is weak in the mean, therefore, the corresponding dissipation source term is linear in the wave spectrum.

Assuming that there is a large separation between the length scale of the waves and the whitecaps the power  $m$  of the wave number in the dissipation source term is found to be equal to 1. However, for the high-frequency part of the wave spectrum such a large gap between waves and whitecaps may not exist, allowing the possibility of a different dependence of the dissipation on wave number.

We finally discuss results of the coupled wave-surface layer model with  $\beta = 2.6$ ,  $m = 2$  and we investigate the dependence of the results on the magnitude of  $\alpha$  (measuring the effect of waves on the shape of the wind profile). We performed two numerical experiments with  $\alpha = 0.1$  and  $\alpha = 0.4$  and from the figures 6–8 we infer that coupling has a significant impact on the results for wave height, whereas owing to the modified dissipation source term a satisfactory behaviour of wave-induced stress and Phillips constant  $\alpha_p$  as function of duration is found. In accord with one's expectations, young wind sea (corresponding to  $T < 6$  h) shows a strong coupling between wind and waves, whereas for old wind sea there is hardly any coupling. For  $\alpha = 0$  (results not shown) the coupling between wind and waves would be even stronger, so that we conclude that it is important to take into account the effect of waves on the shape of the wind profile to obtain reliable estimates for the stress in the surface layer over ocean waves.

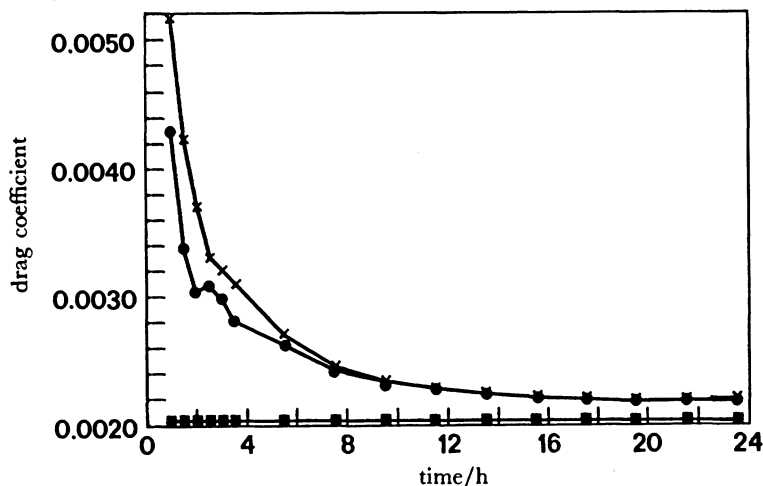


FIGURE 9. Drag coefficient as a function of time. Symbols: ■, standard WAM; ×, coupled ( $\alpha = 0.1$ ); ●, coupled ( $\alpha = 0.4$ ).

Lastly we show the impact of the sea states on the aerodynamic drag in figure 9. Evidently, the standard WAM run shows no dependence of the drag on duration, whereas the runs with the coupled model give a considerable variation in drag with time, because the drag depends on the sea state through the wave-induced stress  $\tau_w$ .

#### 4. CONCLUSIONS AND DISCUSSION

In this paper we have discussed the effect of wind-generated gravity waves on the air flow. Especially for young wind sea, when the wave-induced stress is a large fraction of the total stress in the surface layer, the waves will affect the shape of the wind profile thereby partly quenching the momentum transfer from wind to waves.

For a given wave spectrum, steady-state calculations of the wind profile over ocean waves

show that for young wind sea most of the stress is determined by momentum transfer from wind to waves (i.e. a strong coupling) whereas for old wind sea there is hardly any coupling. We therefore find a strong wave-age dependence of aerodynamic drag on wave age, in agreement with observations.

Next, we allowed the wave spectrum to evolve according to the dynamics of the energy-balance equation. To that end we coupled the WAM model to a simple, steady-state surface-layer model. First results show that a satisfactory behaviour of the wave-induced stress is found provided the dissipation source term in the wave model is modified. Coupling has a significant impact on results for wave height and stress in the surface layer.

In this paper we confined our numerical experiments to the class of dissipation source functions given by equation (27). One might argue that for the high-frequency waves the dissipation is a nonlinear function of the wave-spectrum. Although it is a relatively easy task to do experiments with the latter type of dissipation, guidance from a theory of breaking is clearly desirable. We therefore conclude that a reliable stress determination in the surface layer over ocean waves would clearly benefit from a better knowledge of dissipation due to wave breaking.

Finally, we parametrized the momentum loss of air flow to the short gravity-capillary waves by means of the introduction of the Charnock relation for the roughness length. A more elegant approach is, perhaps, to determine this momentum loss by calculating the gain of momentum of these high-frequency waves. Presently, however, neither a reliable spectral shape nor a reliable expression for the wind input to these short waves is known.

We acknowledge stimulating discussions with Gerbrand J. Komen.

#### REFERENCES

- Banner, M. 1988 On the equilibrium spectrum of wind waves. (Preprint.)
- Birch, K. G. & Ewing, J. A. 1986 *Observations of wind waves on a reservoir*. IOS-report no. 234. (37 pages.)
- Charnock, H. 1955 Wind stress on a water surface. *Q. Jl R. met. Soc.* **81**, 639–640.
- Donelan, M. 1982 The dependence of the aerodynamic drag coefficient on wave parameters. In *Proceeding of the First International conference on Meteorology and Air/Sea Interaction of the Coastal Zone, The Hague, The Netherlands*, pp. 381–387.
- Fabrikant, A. L. 1976 Quasilinear theory of wind-wave generation. *Izv. atmos. ocean. Phys.* **12**, 524.
- Forristal, G. Z. 1981 Measurements of a saturated range in ocean wave spectra. *J. geophys. Res.* **86**, 8075–8084.
- Hasselmann, K., Barnett, T. P., Bouws, E., Carlson, H., Cartwright, D. E., Enke, K., Ewing, J. A., Gienapp, H., Hasselmann, D. E., Meerburg, A., Müller, P., Olbers, D. J., Richter, K., Sell, W. & Walden, H. 1973 Measurements of wind-wave growth and swell decay during the Joint North Sea Wave Project (JONSWAP). *Deutsche Hydrog. Z. suppl. A* (**80**), no. 12.
- Hasselmann, K. 1974 On the spectral dissipation of ocean waves due to whitecapping. *Boundary-Layer Met.* **6**, 107–127.
- Hasselmann, S., Hasselmann, K., Allender, J. H. & Barnett, T. P. 1985 Computations and parametrisations of the nonlinear energy transfer in a gravity-wave spectrum Part II. Parametrisations of the nonlinear transfer for application in wave models. *J. phys. Oceanogr.* **15**, 1378–1391.
- Janssen, P. A. E. M. 1982 Quasilinear approximation for the spectrum of wind-generated water waves. *J. Fluid Mech.* **117**, 493–506.
- Janssen, P. A. E. M. 1989 Wave-induced stress and the drag of air flow over sea waves. *J. phys. Oceanogr.* **19**.
- Komen, G. J., Hasselmann, S. & Hasselmann, K. 1984 On the existence of a Fully Developed Wind-sea Spectrum. *J. phys. Oceanogr.* **14**, 1271–1285.
- Komen, G. J. 1985 Energy and momentum fluxes through the sea surface. In *Dynamics of the ocean surface mixed layer* (ed. P. Müller & D. Henderson). Proceedings 'Aha Huliko'a', 14–16 Jan. Hawaii Institute of Geophysics special publication, 1987, pp. 207–217.
- Miles, J. W. 1957 On the generation of surface waves by shear flows. *J. Fluid Mech.* **3**, 185.

- Miles, J. W. 1965 A note on the interaction between surface waves and wind profiles. *J. Fluid Mech.* **22**, 823–827.
- Snyder, R. L. 1974 A field study of wave-induced pressure fluctuation above surface gravity waves. *J. mar. Res.* **32**, 497–531.
- Snyder, R. L., Dobson, F. W., Elliot, J. A. & Long, R. B. 1981 Array measurements of atmospheric pressure fluctuations above surface gravity waves. *J. Fluid Mech.* **102**, 1.
- The WAMDI-group: Hasselmann, S., Hasselmann, K., Bauer, E., Janssen, P. A. E. M., Komen, G. J., Bertotti, L., Lionello, P., Guillaume, A., Cardone, V. C., Greenwood, J. A., Reistad, M., Zambresky, L. & Ewing, J. A. 1988 The WAM model – a third generation ocean wave prediction model. *J. phys. Oceanogr.* **18**, 1775–1810.
- Wu, J. 1982 Wind-stress coefficients over sea surface from breeze to hurricane. *J. geophys. Res.* **87**, 9704–9706.